Measurement of the ratio $B(D^0 \to K^{*-} e^+ \nu_e)/B(D^0 \to K^- e^+ \nu_e)$

G. Crawford,[a] R. Fulton,[a] K. K. Gan,[a] T. Jensen,[a] D. R. Johnson,[a] H. Kagan,[a]
R. Kass,[a] R. Malchow,[a] F. Morrow,[a] J. Whitmore,[a] P. Wilson,[a] D. Bortoletto,[b] D. Brown,[b]
J. Dominick,[b] R. L. McIlwain,[b] D. H. Miller,[b] M. Modesitt,[b] C. R. Ng,[b] S. F. Schaffner,[b] E. I. Shibata,[b]
I. P. J. Shipsey,[b] M. Battle,[c] P. Kim,[c] H. Kroha,[c] K. Sparks,[c] E. H. Thorndike,[c] C.-H. Wang,[c]
M. S. Alam,[d] I. J. Kim,[d] B. Nemati,[d] V. Romero,[d] C. R. Sun,[d] P.-N. Wang,[d] M. M. Zoeller,[d]
M. Goldberg,[e] T. Haupt,[e] N. Horwitz,[e] V. Jain,[e] Rosemary Kennett,[e] M. D. Mestayer,[e] G. C. Moneti,[e]
Y. Rozen,[e] P. Rubin,[e] T. Skwarnicki,[e] S. Stone,[e] M. Thusalidas,[e] W.-M. Yao,[e] G. Zhu,[e]
A. V. Barnes,[f] J. Bartelt,[f] S. E. Csorna,[f] T. Letson,[f] J. Alexander,[g] M. Artuso,[g] C. Bebek,[g]
K. Berkelman,[g] D. Besson,[g] T. Browder,[g] D. G. Cassel,[g] E. Cheu,[g] D. M. Coffman,[g] P. S. Drell,[g]
R. Ehrlich,[g] R. S. Galik,[g] M. Garcia-Sciveres,[g] B. Geiser,[g] B. Gittelman,[g] S. W. Gray,[g] D. L. Hartill,[g]
B. K. Heltsley,[g] K. Honscheid,[g] J. Kandaswamy,[g] N. Katayama,[g] D. L. Kreinick,[g] J. D. Lewis,[g] G. S. Ludwig,[g]
J. Masui,[g] J. Mevissen,[g] N. B. Mistry,[g] S. Nandi,[g] E. Nordberg,[g] C. O'Grady,[g] J. R. Patterson,[g]
D. Peterson,[g] M. Pisharody,[g] D. Riley,[g] M. Sapper,[g] M. Selen,[g] A. Silverman,[g] H. Worden,[g]
M. Worris,[g] A. J. Sadoff,[h] P. Avery,[i] A. Freyberger,[i] J. Rodriguez,[i] J. Yelton,[i] S. Henderson,[j]
K. Kinoshita,[j] F. Pipkin,[j] M. Procario,[j] M. Saulnier,[j] R. Wilson,[j] J. Wolinski,[j] D. Xiao,[j]
H. Yamamoto,[j] R. Ammar,[k] P. Baringer,[k] D. Coppage,[k] R. Davis,[k] P. Haas,[k] M. Kelly,[k]
N. Kwak,[k] H. Lam,[k] S. Ro,[k] Y. Kubota,[l] J. K. Nelson,[l] D. Perticone,[l] R. Poling,[l] and
S. Schrenk[l]

(CLEO Collaboration)

[a]*Ohio State University, Columbus, Ohio 43210*
[b]*Purdue University, West Lafayette, Indiana 47907*
[c]*University of Rochester, Rochester, New York 14627*
[d]*State University of New York at Albany, Albany, New York 12222*
[e]*Syracuse University, Syracuse, New York 13244*
[f]*Vanderbilt University, Nashville, Tennessee 37235*
[g]*Cornell University, Ithaca, New York 14853*
[h]*Ithaca College, Ithaca, New York 14850*
[i]*University of Florida, Gainesville, Florida 32611*
[j]*Harvard University, Cambridge, Massachusetts 02138*
[k]*University of Kansas, Lawrence, Kansas 66045*
[l]*University of Minnesota, Minneapolis, Minnesota 55455*

(Received 10 May 1991)

Using the CLEO detector at the Cornell Electron Storage Ring, we have performed a direct measurement of the ratio of D^0 semileptonic branching fractions into vector and pseudoscalar final states. We find $B(D^0 \to K^{*-} e^+ \nu_e)/B(D^0 \to K^- e^+ \nu_e) = 0.51 \pm 0.18 \pm 0.06$, in agreement with the ratio derived by the E691 experiment which compares D^+ and D^0 final states. We also set an upper limit on the ratio $B(D^0 \to \bar{K}^{*0} \pi^- e^+ \nu_e)/B(D^0 \to K^{*-} e^+ \nu_e) < 0.64$ at 90% confidence level.

I. INTRODUCTION

Theoretical models of semileptonic D meson decay [1,2] have been brought into question following the E691 measurement of the ratio $\Gamma(D \to K^* e^+ \nu_e)/\Gamma(D \to K e^+ \nu_e)$ as $0.45 \pm 0.09 \pm 0.07$, because the models prefer a value of one greater. In addition, E691 found a K^* polarization much larger than predicted [3]. To obtain these results E691 analyzed the decay $D^+ \to K^{*0} e^+ \nu_e$ for the vector final state and $D^0 \to K^- e^+ \nu_e$ for the pseudoscalar final state. They used their well-measured ratio of D lifetimes and absolute branching fractions from Mark III to determine the ratio of partial widths. In a recent paper the Mark III group reports a larger vector/pseudoscalar ratio, 0.93 ± 0.28 [4], but the error is large enough to accommodate both the theoretical expectations and the E691 result.

Here we present a new result for the ratio of exclusive branching fractions. In this analysis, we determine the ratio of branching fraction directly from the observed number of events in the modes $D^0 \to K^{*-} e^+ \nu_e$ and $D^0 \to K^- e^+ \nu_e$, avoiding any dependence on absolute branching-ratio normalizations.

II. DATA SAMPLE AND DETECTOR DESCRIPTION

The data were taken with the CLEO detector at the Cornell Electron Storage Ring (CESR) from September

1986 to March 1988. Data were collected at $\Upsilon(3S), \Upsilon(4S), \Upsilon(5S)$ and the continuum 60 MeV below the $\Upsilon(4S)$. The total integrated luminosity is 490 pb^{-1}. The CLEO detector is described in detail elsewhere [5]. This analysis uses the central tracking chamber and the electron and muon identification systems. The momentum resolution for charged particles is

$$(\delta p/p)^2 = (0.0023p)^2 + (0.007)^2, \text{ with } p \text{ in GeV}/c \ .$$

Electrons are identified using a 12-radiation-length-thick lead plate-proportional chamber calorimeter and dE/dx information from the main drift chamber. The calorimeter fiducial volume is $0.47(4\pi)$, while the dE/dx information is available over $0.9(4\pi)$. The resolution of the calorimeter is $\sigma_E/E = 0.21/\sqrt{E\ /(\text{GeV})}$, while the dE/dx resolution is 6.5%. Muons are identified using information from proportional wire chambers placed inside and outside of steel plates which are 1.0 to 1.5 meters in thickness. The fiducial solid angle is $0.76(4\pi)$.

The event sample is selected by using standard CLEO hadronic event selection [6]. To suppress the background from $\Upsilon(3S)$, $\Upsilon(4S)$, and $\Upsilon(5S)$ resonance decays, we require the ratio of the Fox-Wolfram moments [7], $R_2 = H_2/H_0 \geq 0.33$. R_2 is calculated using charged tracks only.

Since we are concerned here with semileptonic decays we need to find electrons and muons. Electrons below 1.0 GeV/c are not used in this analysis. Electrons with momenta between 1.0 and 1.4 GeV/c are identified only if they are within the calorimeter fiducial volume. Information from both the calorimeter and dE/dx systems is used. Electrons above 1.4 GeV/c are identified outside the calorimeter fiducial volume using only the dE/dx system or are identified inside the calorimeter fiducial volume using both systems. The efficiency for identifying electrons within the calorimeter fiducial volume is 85%, whereas the identification efficiency outside this volume is about 60%. The average probability of misidentifying a hadron as an electron, over the relevant momentum range, is roughly 0.4% inside the calorimeter fiducial volume and 0.8% outside. A track with measured momentum greater than 1.4 GeV/c is labeled as a muon candidate if it penetrates all of the steel and registers hits in the orthogonal layers of the outer muon chambers [8]. The muon identification efficiency (within the muon fiducial volume) increase from 24% at 1.4 GeV/c, to 79% at 2.0 GeV/c and stays constant beyond. The average probability for misidentifying a hadron as a muon increases from 0.8% at 1.4 GeV/c to 1.4% at 2.0 GeV, and stays constant beyond.

III. DETECTION OF $D^0 \to K^{*-} e^+ \nu_e$

D^0's are required to be decay products of D^{*+}'s from the reaction $D^{*+} \to D^0 \pi^+$. D^{*+} candidates are formed from three-body combinations containing a π^+, a e^+, and, in this case, a K^{*-}, where the $K^{*-} \to K_S^0 \pi^-$. We also look for the charge-conjugate reaction. (In this paper, unless otherwise stated use of the charge-conjugate reaction is implicit.) To select K_S^0 candidates we search for two tracks of opposite charge which intersect in the plane transverse to the beam direction at least 2 mm away from the main event vertex. The invariant mass of these two tracks, assumed to be pions, is required to lie within ± 20 MeV (approximately 5σ) of the nominal value of the K_S mass.

We now have selected three of the four particles from the D^{*+} decay. Only the neutrino is missing. To proceed further we impose additional selection criteria on our candidate sample. First we estimate the D^0 momentum. We assume that the parent D^{*+} goes along the thrust axis which is calculated using all the charged tracks in the event; and, since the magnitude of the pion momentum in the D^{*+} rest frame is known, and its momentum in the laboratory frame can be measured, we can calculate the boost necessary to give the π^+ its measured momentum, and thus find the D^0 momentum (see the Appendix for the necessary equations). In general there is a twofold ambiguity, due to the fact that the pion can travel either forward or backward with respect to the D^{*+} direction. At times, one of the solutions is unphysical, due to approximations made in the calculation, and can be discarded. If both solutions are allowed, we choose the solution where the D^0 is traveling forward with respect to the D^{*+} direction. In Fig. 1, we show the ratio of the generated (D^0) momentum to the reconstructed momentum. This technique improves with increasing D^0 (or D^{*+}) momentum.

In order to improve the purity of the $D^0 \to K^{*-} e^+ \nu_e$ signal additional requirements are imposed. (1) The K^{*-} momentum must be greater than 0.7 GeV/c. (2) The invariant mass of K^{*-} and the electron must be less than

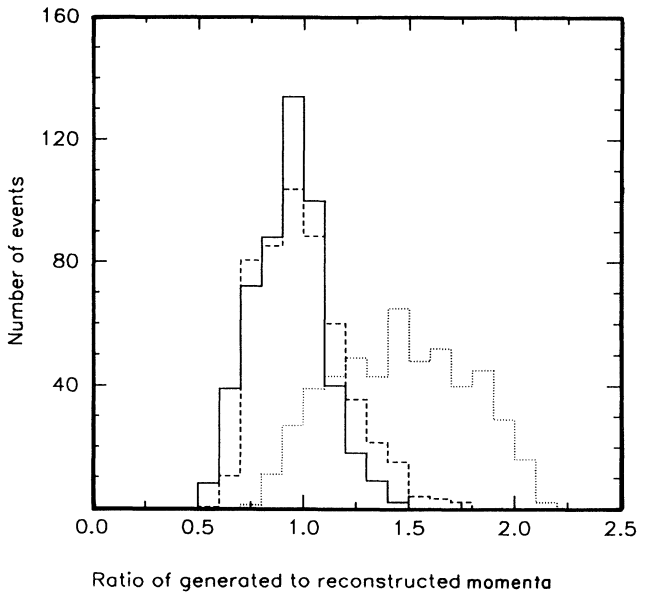

FIG. 1. Ratio of generated to reconstructed momenta for D^0 (the detector response is ignored for these Monte Carlo events): solid line is for the case where there is only one physical solution; dashed line is for the case where the D^0 is traveling forward with respect to the D^{*+} direction; and the dotted line is for the D^0 traveling backwards with respect to the D^{*+} direction.

1.9 GeV. This is always true for real D^0 decays. (3) The momentum of the D^0, found by solving Eq. (A5) of the Appendix, must be above 2 GeV/c. (4) We construct a pseudo D^{*+} mass by calculating the invariant mass of the K^{*-}, the electron, and the π^+, and a pseudo D^0 mass by calculating the invariant mass of the K^{*-} and the electron. The pseudomass difference between the D^{*+} and the D^0 must lie between 140 and 200 MeV. The mass difference between real D^0 and D^{*+} candidates is known to be 145.45±0.07 MeV. The width of the cut accounts for the smearing from the missing neutrino.

The $K_S^0\pi^-$ mass distribution is fitted with a Breit-Wigner line shape, shown in Fig. 2. The mass and width of the K^{*-} are fixed to be 0.892 GeV and 55 MeV, respectively, which are consistent with Monte Carlo simulation of the detector. The fit yields 54±12 K^{*-}'s. The systematic error on the signal is small compared to the statistical error. For instance, if we let the mass and the width of the K^{*-} float, the yield changes by less than 3 events. To find a branching ratio we need to correct the K^{*-} yield for detection efficiency and to estimate the background in the sample.

The detection efficiency is determined by dividing the number of detected events, determined from a Monte Carlo simulation, to the total number of generated D^{*+} [9]. Semileptonic decays are generated according to the Isgur model [10,11]. Longitudinally and transversely polarized K^{*-} are simulated and analyzed separately. We find that the efficiency for the longitudinally polarized state is 0.95% while that for the transverse state is 0.85%. Included in the efficiency are branching fractions for decays of K^{*-} and K_S to observable particles; since all our D^0's are tagged by the $D^{*+}\to D^0\pi^+$ decay we do not include this branching ratio, but have included the efficiency to detect the π^+. We assume the ratio of longitudinally polarized to transversely polarized K^{*-} to be 1.1, as specified in the Isgur model, for the overall efficiency which is listed in Table I [12].

There are several sources of background which could be in our sample. These include fake electrons, random K^{*-}-positron combination from $B\bar{B}$ events, and random K^{*-}-positron combinations from continuum events. We evaluate the background due to fake electrons by repeating the analysis, but treating all charged tracks in the electron fiducial volume as candidate electrons. The K^* mass distribution is fitted separately in each charged-track momentum bin, to get the number of K^*-electron combinations in each bin. We then multiply this number by the probability of a charged track faking an electron. The background due to random K^*-positron combinations from $B\bar{B}$ events, which is suppressed by the R_2 cut, is determined by processing generic ($B\bar{B}$) Monte Carlo events through the same analysis chain as the data [13]. Another source of background is due to the combination of random K^{*-} and e^+ from continuum events. The size of this effect is found by generating continuum Monte Carlo events and determining how many random candidates satisfy our cuts. The resulting background estimates are also given in Table I. The systematic error includes the uncertainty in the background estimates, electron identification efficiency, and the difference in the Monte Carlo efficiency for detecting longitudinal and transverse polarizations [14].

We have checked our background estimates by using

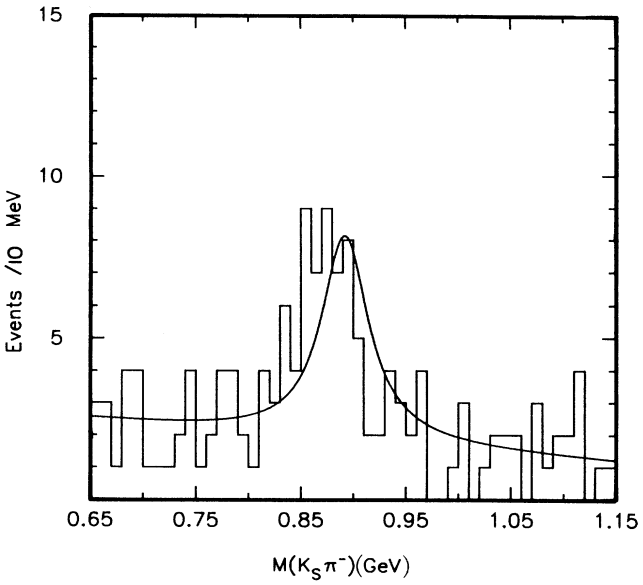

FIG. 2. The histogram is the $K_S^0\pi^-$ candidate mass for the decay mode $D^0\to K^{*-}e^+\nu_e$. The solid line is a fit to the data using a Breit-Wigner line shape for the signal and a first-order polynomial for the background.

TABLE I. Number of signal and background events.

Quantity	Number of events
Number of K^{*-} in data sample	54.0±12.0
Background from electron fakes	6.0±0.2±1.6
Background from $B\bar{B}$ events	6.0±2.4±3.0
Background from random K^{*-}-e^+ combinations in continuum events	5.0±0.7±2.0
Net yield	37.0±12.3±4.0
Efficiency	(0.9±0.1)%
Corrected yield	4111±1366±610

the same techniques to predict the number of wrong-sign events. Here wrong sign is defined as $D^{*+}\to D^0\pi^+$, $D^0\to K^{*+}e^-\bar{\nu}_e$. Note that the sign of K^* and the electron are reversed with respect to the charge of the pion emitted by the D^{*+}. We predict that there should be 13 ± 4 events. We actually observe 19 ± 9 wrong-sign events, consistent with our expectations.

IV. DETECTION OF $D^0\to(K^*\pi)^-e^+\nu_e$

In the above analysis, the final state could contain an extra π^0, which remains undetected. To measure the level of contamination from $D^0\to K^{*-}e^+\pi^0\nu_e$, we search for the mode $D^0\to\bar{K}^{*0}\pi^-e^+\nu_e$, $\bar{K}^{*0}\to K^-\pi^+$, and relate it to the final state $K^{*-}\pi^0e^+\nu_e$. The dE/dx pulse height for the kaon candidate is required to be within 2 standard deviations of that expected for a kaon. The kinematic cuts and the cuts on the electron momentum and R_2 applied to the $\bar{K}^{*0}\pi^-e^+$ system are the same as those previously described for $K^{*-}e^+$.

The K^{*0} mass distribution for events passing these cuts is fitted to a Breit-Wigner line shape. The fit yields 9 ± 7 events. The generic $B\bar{B}$ Monte Carlo simulation did not yield any background events. We take the conservative approach of not subtracting electron fakes or random $K^{*-}\pi^0$-electron combinations. We set an upper limit of <18.4 events at 90% confidence level.

Since the production mechanism for the $(\bar{K}^{*0}\pi^-)$ system is unknown, we need to choose a model in order to determine the detection efficiency. We choose $D^0\to K_1(1270)^-\ e^+\nu_e$, where $K_1(1270)^-\to\bar{K}^{*0}\pi^-$. This choice is made because $K_1(1270)^-$ is the lowest-mass strange resonance which can produce the $\bar{K}^{*0}\pi^-$ system. The efficiency for detecting this mode is $0.7\pm0.1\%$. We also generated the $\bar{K}^{*0}\pi^-e^+\nu_e$ final state according to phase space and found that the resulting efficiency is the same as found for the other model.

Even though we do not see a signal, for use in further computations we quote the ratio of branching fractions to be

$$\frac{B(D^0\to K^{*0}\pi^-e^+\nu_e)}{B(D^0\to K^{*-}e^+\nu_e)}=0.31\pm0.24\ , \tag{1}$$

which gives an upper limit of 0.64 at 90% confidence level.

Assuming that the $K^*\pi$ system is a state with isospin $\frac{1}{2}$, the $K^{*-}\pi^0$ state will be produced with one-half the strength as the $K^{*0}\pi^-$ state that we have searched for. This is true irrespective of whether the $K^*\pi$ state is produced resonantly or nonresonantly. Thus, based on the equation (1), we compute the ratio

$$\frac{B(D^0\to K^{*-}\pi^0e^+\nu_e)}{B(D^0\to K^{*-}e^+\nu_e)}=0.16\pm0.12\ , \tag{2}$$

which gives a 90% confidence level upper limit of 0.32. Most of the systematic errors cancel when the ratios in Eqs. (1) and (2) are computed.

In principle, there could be contamination from $D^0\to K^{*-}\pi^0e^+\nu_e$ in the $D^0\to K^{*-}e^+\nu_e$ sample. Using the observed upper limit on the number of events in the $K^*\pi$ search and evaluating the efficiencies of detecting $K^{*-}\pi^0e^+\nu_e$ as a pure $K^{*-}e^+\nu_e$ final state, we find that this contamination is $<22\%$ at 90% confidence level. We proceed by making the assumption that the $K^{*-}\pi^0e^+\nu_e$ final state is negligible [15].

V. DETECTION OF $D^0\to K^-l^+\nu$

We now describe the search for $D^0\to K^-e^+\nu_e$ and $D^0\to K^-\mu^+\nu_\mu$. We use selection criteria similar to those used for the K^{*-} final state. (1) We require that the cosine of the angle between the kaon and the lepton in the laboratory frame be greater than zero, instead of requiring a minimum kaon momentum. (2) The K^--lepton invariant mass M_{K^-l} must be less than 1.9 GeV. (3) The momentum of the D^0, found by solving Eq. (A5) of the Appendix, must be above 2 GeV/c. (4) The pseudo D^{*+} mass cut, $140<M_{D^0\pi^+}-M_{D^0}<200$ MeV, must be satisfied, where the M_{D^0} is now taken to be M_{K^-l}. (5) The kaon candidate must have a dE/dx pulse height within 2 standard deviations of that expected for a kaon.

In addition, to reduce the background from $D^0\to K^{*-}l^+\nu$ (see below), we calculate the missing mass squared M_ν^2 defined as $(P_D-P_l-P_K)^2$, where the P_x's are the four-vectors for the D, lepton, and kaon, respectively. The Monte Carlo missing-mass plot for the pseudoscalar/vector final states is shown in Fig. 3, while Fig. 4 shows the corresponding plot for the electronic mode. Therefore, we impose the final requirement that $-2.0\ \text{GeV}^2<M_\nu^2<0.5\ \text{GeV}^2$. There is no substantial systematic error involved in counting the number of events which pass these cuts.

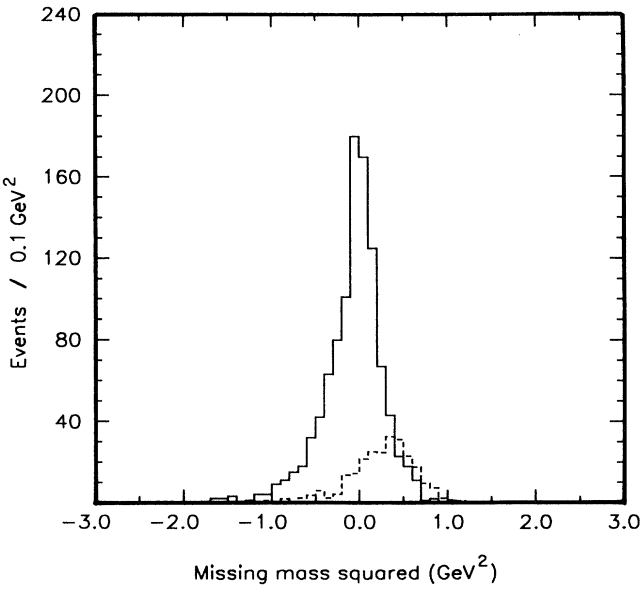

FIG. 3. Missing-mass (Monte Carlo events) plot for $D^0\to K^-e^+\nu_e$ (solid) and for $D^0\to K^{*-}e^+\nu_e$, $K^{*-}\to K^-\pi^0$ (dashed).

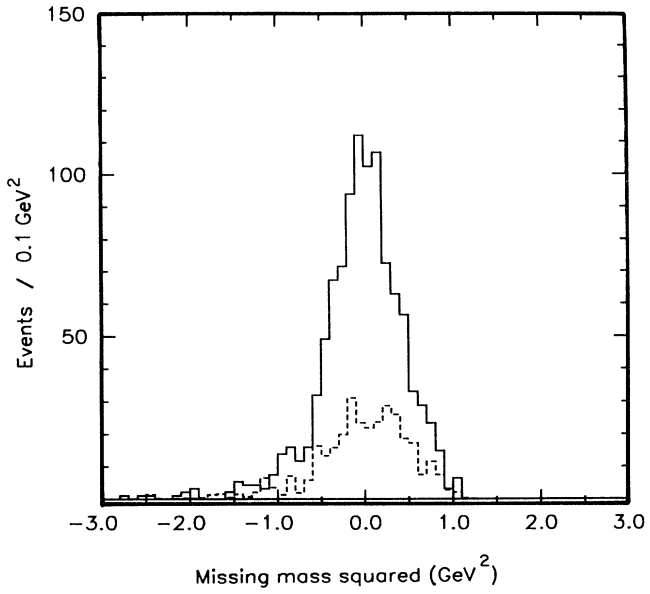

FIG. 4. Missing-mass plot for $D^0 \to K^- e^+ \nu_e$. Solid histogram is the raw data; dashed histogram is the expected background.

Next we estimate the backgrounds in this channel. To find the number of lepton fakes, we form M_ν^2 using all charged tracks, taken in turn, in the lepton fiducial volume. This is done in various momentum bins, as the lepton fake rate is momentum dependent. We then count the number of combinations passing the above cuts and multiply by the probability of a track faking a lepton. The results are listed in Table II. Also shown in the table is the estimated background due to random K^--lepton combinations from $B\bar{B}$ events, again determined by processing generic ($B\bar{B}$) Monte Carlo events through the same analysis chain as the data.

Another source of background is due to the random combination of misidentified pions (or random kaons) and leptons from continuum events. This effect is studied by comparing Monte Carlo efficiencies for detecting $K^- l^+ \nu$ events when we use only the daughter K^- for reconstructing the final state against the case when we use all tracks passing the dE/dx cut for the kaon candidate. We estimate this background to be about 13% of the observed sample (this number is roughly the same for the electronic and muonic modes). Again, the results can be found in Table II.

We also need to consider the background from the decay $D^0 \to K^{*-} l^+ \nu$, where $K^{*-} \to K^- \pi^0$ and the π^0 is undetected. The efficiency for detecting $D^0 \to K^{*-} e^+ \nu_e$ as $D^0 \to K^- e^+ \nu_e$ is determined to be 20% (the corresponding number for the muonic mode is 16%). The numbers of background events are listed in Table II.

To check our background estimates, we predict the number of wrong-sign events that should be observed, where the wrong sign in this case is $D^{*+} \to D^0 \pi^+$, $D^0 \to K^+ l^- \nu$; i.e., the sign of K and lepton are reversed with respect to the charge of the pion emitted by the D^{*+}. There are 282±17 (175±13) wrong-sign events, as compared to our estimate of 262±35 (184±30) events for the electronic (muonic) mode [16].

Table II summarizes the numbers of events in the signal and background and also contains the detection efficiencies for both electronic and muonic modes. The detection efficiency is determined using the Isgur model [10,11]. The systematic error includes the uncertainty in the background estimates, lepton identification, and in the Monte Carlo efficiency.

VI. DETERMINATION OF $B(D^0 \to K^{*-} e^+ \nu_e)/B(D^0 \to K^- e^+ \nu_e)$

By comparing the net yields for the $D^0 \to K^{*-} e^+ \nu_e$ and $D^0 \to K^- e^+ \nu_e$ modes and correcting by the relative efficiencies, the ratio of branching fractions is directly determined. We find

$$\frac{B(D^0 \to K^{*-} e^+ \nu_e)}{B(D^0 \to K^- e^+ \nu_e)} = 0.51 \pm 0.18 \pm 0.06 \ . \tag{3}$$

The systematic error on this ratio is obtained by combining the systematic error on the yields of the numerator and the denominator. Contamination from the reaction $D^0 \to (K^* \pi)^- e^+ \nu_e$ could change this ratio. To evaluate this possible effect we use the ratio found in Eq. (1) and Monte Carlo–generated detection efficiencies for this mode to contaminate both the $K^{*-} e^+ \nu_e$ and $K^- e^+ \nu_e$ final states. We need to consider the contamination from

TABLE II. Events and efficiencies for the $K^- l^+ \nu$ mode.

Quantity	Electrons	Muons
Number of K^-	914±30	440±21
Background from random K-l combinations and pions misidentified as kaons	140±11±21	51±7±8
Background from lepton fakes	90±1±21	121±2±24
Background from $B\bar{B}$ events	43±6±21	18±4±9
Background from $K^{*-} l^+ \nu$	57±18±15	19±6±5
Net yield	584±37±39	231±23±27
Efficiency for $K^- l^+ \nu$	(7.2±0.2)%	(3.2±0.2)%
$B(D^0 \to K^- l^+ \nu)$	3.8±0.3±0.6%	3.3±0.3±0.6%

both $K^{*-}\pi^0e^+\nu_e$ and $K^{*0}\pi^-e^+\nu_e$. The efficiency for $K^{*-}\pi^0e^+\nu_e$ to fake $K^{*-}e^+\nu_e$ is 70%, while the efficiency for $K^{*0}\pi^-e^+\nu_e$ to fake $K^{*-}e^+\nu_e$ is zero. This results in a net contamination of $11\pm8\%$. The efficiencies for each of the $(K^*\pi)^-e^+\nu_e$ states to fake $K^-e^+\nu_e$ are about 12%. Using the ratio of branching ratios found in Eq. (3), we find that the possible contamination in the $K^-e^+\nu_e$ mode due to this source is $1.4\pm0.7\%$.

The effect of including this possible effect is to lower the vector/pseudoscalar ratio in Eq. (3) to 0.45, increasing the disagreement with theory.

VII. EXCLUSIVE BRANCHING FRACTIONS

We now determine the absolute branching fractions for the $D^0\to K^-l^+\nu$, $K^{*-}e^+\nu_e$, and $(K^*\pi)^-e^+\nu_e$ final states. For the electronic (and muonic) modes of the pseudoscalar final state we measure the branching ratio relative to the $D^0\to K^-\pi^+$ mode. We find $B(D^0\to K^-e^+\nu_e)/B(D^0\to K^-\pi^+)=0.9\pm0.06\pm0.06$. Using the Mark III result [17] that $B(D^0\to K^-\pi^+)$ equals $4.2\pm0.4\pm0.4\%$, yields $B(D^0\to K^-e^+\nu_e)=3.8\pm0.3\pm0.6\%$. The systematic error [16] includes uncertainties in the detection efficiency, in the background estimates, and in the $D^0\to K^-\pi^+$ branching ratio.

In Table II, we also present the results for the muonic mode. Since we did not measure the corresponding mode for the vector final state, these data are used only for the determination of the exclusive branching ratio. The missing-mass plot is shown in Fig. 5. Following the same procedure as in the case of the electronic mode, we find $B(D^0\to K^-\mu^+\nu_\mu)/B(D^0\to K^-\pi^+)=0.79\pm0.08\pm0.09$, and $B(D^0\to K^-\mu^+\nu_\mu)=3.3\pm0.3\pm0.6\%$.

The branching ratio for $D^0\to K^{*-}e^+\nu_e$ is obtained by normalizing to $D^0\to K^{*-}\pi^+$ decay mode. The advantage of using this mode is that we cancel out systematic

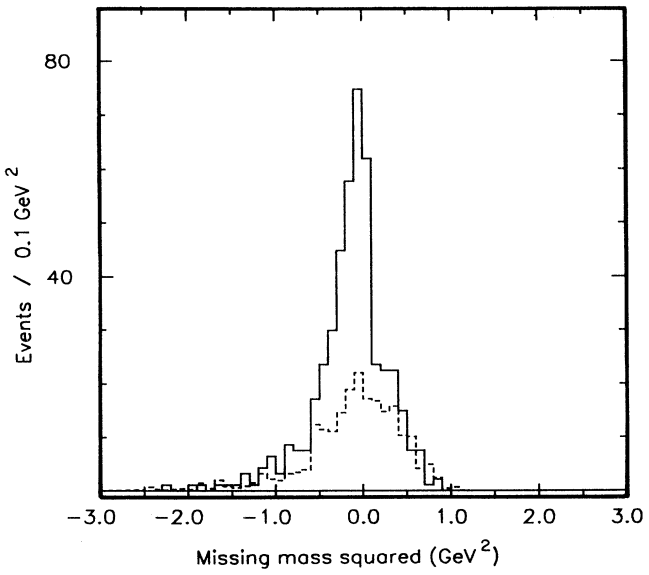

FIG. 5. Missing-mass plot for $D^0\to K^-\mu^+\nu_\mu$. Solid histogram is for the raw data sample; dashed histogram is the expected background.

effects in our algorithm to tag K^{*-}'s. We find $B(D^0\to K^{*-}e^+\nu_e)/B(D^0\to K^{*-}\pi^+)=0.36\pm0.12\pm0.05$. Using the Mark III result [19] that $B(D^0\to K^{*-}\pi^+)$ equals $(5.2\pm1.0)\%$, we obtain $B(D^0\to K^{*-}e^+\nu_e)=(1.9\pm0.6\pm0.5)\%$. The systematic error includes the uncertainties in the efficiency, background estimates, and in the branching ratio for $D^0\to K^{*-}\pi^+$.

For the $D^0\to\bar{K}^{*0}\pi^-e^+\nu_e$ decay mode, we obtain the 90% confidence level upper limit:

$$\frac{B(D^0\to\bar{K}^{*0}\pi^-e^+\nu_e)}{B(D^0\to K^{*-}\pi^+)}<0.23\ .$$

Using the Mark III branching ratio for $D^0\to K^{*-}\pi^+$, we get $B(D^0\to\bar{K}^{*0}\pi^-e^+\nu_e)<1.2\%$ at 90% confidence level. This gives an upper limit for $B(D^0\to K^{*-}\pi^0e^+\nu_e)<0.6\%$ at 90% confidence level. These results are consistent with a previous result [4], where the branching ratio for D^0 semileptonic decays in excess of pseudoscalar and vector modes (K^-,$K^{*-}\pi^-\rho^-$) was an inconclusive $0.7\pm1.1\%$.

VIII. HADRONIC STRUCTURE OF $D^0\to K^-e^+\nu_e$ DECAYS

We investigate the hadronic structure of $D^0\to K^-e^+\nu_e$, by studying the q^2 distribution, where q^2 is the square of the four-momentum transferred to the $e^+\nu_e$ system $[q^2=(P_D-P_K)^2]$. Theoretical models parametrize this decay by one form factor. The single pole form is common, and is expressed as

$$f_+(q^2)=\frac{f_+(0)}{1-q^2/M_p^2}\ ,$$

where M_p is the pole mass. For the $c\to s$ transition, the pole mass is expected to be 2.11 GeV (mass of D_s^*).

To measure M_p we generate Monte Carlo events, according to the model of Körner and Schuler [2], for values of M_p ranging from 1.5 to 2.7 GeV, and process them through the analysis chain. We fit the resulting Monte Carlo q^2 distributions to the data, where the background has been subtracted from the latter as a function of q^2, and determined the χ^2. The minimum χ^2 yields the pole mass $M_p=2.0^{+0.4+0.3}_{-0.2-0.2}$ GeV. The systematic error is obtained by varying the amount of background [21] subtracted from the raw q^2 distribution by ±1 standard deviation (σ), where σ is the total systematic error on the background. This determination is consistent with previous measurements [20,4].

Assuming the pole mass to be the D_s^* mass, one can write [22]

$$\Gamma(D^0\to K^-e^+\nu_e)=|V_{cs}|^2f_+(0)|^2(1.54\times10^{11})s^{-1}\ .$$

Using the branching ratio determined above and the measured D^0 lifetime [18], we determine $|V_{cs}|^2|f_+(0)|^2$ to be $0.62\pm0.05\pm0.09$. Assuming $|V_{cs}|=|V_{ud}|=0.975$ [18], yields $|f_+(0)|=0.81\pm0.03\pm0.06$. Theoretical models [23] predict $|f_+(0)|$ to lie between 0.6 and 0.82.

IX. SUMMARY AND CONCLUSIONS

In Table III we present our results for the exclusive D^0 decay modes and compare them with the total D^0 semileptonic decay width. We use the Mark III [25] results for the $D^0 \to e^+ X$ inclusive semileptonic branching ratio. We choose this scheme because we use Mark III branching ratios to normalize our results. We have averaged the $K^- e^+ \nu$ and $K^- \mu^+ \nu$ modes taking into account that the branching ratio for the muonic mode is expected to be 96% of the electronic branching ratio, purely due to the difference between electron and muon masses. We ignore nonresonant $K^- \pi^+$ contributions in this table, which have been estimated as $7 \pm 7\%$ of the K^{*-} final state [3]. For the Cabibbo-suppressed modes, we use the theoretical models [24] to predict their width relative to the Cabibbo-favored modes. Although the sum of the exclusive decay rates and the total semileptonic width are consistent within errors, there is room for additional decay modes.

In conclusion we have measured $B(D^0 \to K^{*-} e^+ \nu_e) / B(D^0 \to K^- e^+ \nu_e) = 0.51 \pm 0.18 \pm 0.06$. Our result agrees with the E691 result of $0.45 \pm 0.09 \pm 0.07$ [3], and is in marginal agreement with the Mark III result of 0.93 ± 0.28 [4]. Averaging over the three experiments yields a vector/pseudoscalar ratio of 0.53 ± 0.10, which disagrees with most theoretical models. The corresponding ratio for the B meson [6] $B(B^0 \to D^{*-} l\nu)/B(B^0 \to D^- l\nu)$ is $2.6^{+1.5}_{-1.0}$, which is in agreement with theoretical models [1].

We can compare our measured branching ratio for $D^0 \to K^{*-} e^+ \nu_e$ of $1.9 \pm 0.6 \pm 0.5\%$ with experimental results for $B(D^+ \to K^{*0} e^+ \nu)$ by assuming that the D^+ and D^0 have equal semileptonic widths. E691 and ARGUS [26] have measured values for $B(D^+ \to K^{*0} e^+ \nu)$, from which values of $(1.8 \pm 0.3 \pm 0.2)\%$ and $(1.7 \pm 0.3 \pm 0.4)\%$, respectively, can be derived for $B(D^0 \to K^{*-} e^+ \nu_e)$. These are smaller than the Mark III value of $(4.4^{+1.9}_{-1.0} \pm 0.6)\%$ [4]. We have also measured the electronic and muonic modes for $D^0 \to K^- l\nu$ to be $(3.8 \pm 0.3 \pm 0.6)\%$ and $(3.3 \pm 0.3 \pm 0.6)\%$, respectively. The average of the two gives a rate of $(3.6 \pm 0.3 \pm 0.6)\%$ for the muonic mode and $(3.7 \pm 0.3 \pm 0.6)\%$ for the electronic mode. The largest source of systematic error in these exclusive branching fractions is the uncertainty in the absolute D^0 branching ratios used for normalization. The electronic branching ratio is in agreement with the E691 and Mark III results [3,4]. The branching ratio for the muonic mode is higher than the E653 results of $(2.4 \pm 0.4 \pm 0.5)\%$ [27].

We have searched for $D^0 \to \bar{K}^{*0} \pi^- e^+ \nu_e$, and determine a 90% C.L. upper limit of 1.2%. This is consistent with a previous result [4], where the branching ratio for D^0 semileptonic decays in excess of pseudoscalar and vector modes $(K^-, K^{*-} \pi^- \rho^-)$ was an inconclusive $(0.7 \pm 1.1)\%$.

TABLE III. Summary of D^0 semileptonic decay rates.

Mode	Branching ratio
$D^0 \to K^- e^+ \nu_e$	$3.7 \pm 0.3 \pm 0.6$
$D^0 \to K^{*-} e^+ \nu_e$	$1.9 \pm 0.6 \pm 0.5$
Sum of Cabibbo-favored modes	$5.6 \pm 0.7 \pm 0.8$
Cabibbo-suppressed modes	$0.4 \pm 0.1 \pm 0.1$
Sum of exclusive modes	$6.0 \pm 0.7 \pm 0.8$
$\Gamma(D^0 \to e^+ X)$ measured directly	$7.5 \pm 1.1 \pm 0.4$

ACKNOWLEDGMENTS

We gratefully acknowledge the effort of the CESR staff. P.S.D. thanks the PYI program of the NSF, K.H. thanks the Alexander von Humboldt Stiftung Foundation, and R.P. thanks the A.P. Sloan Foundation for support. This work was supported by the National Science Foundation and the U.S. Department of Energy under Contracts Nos. DE-(AC02[76ER(01428, 03064, 01545), 78ER05001, 83ER-40103], and FG05-86ER40272). The supercomputing resources of the Cornell Theory Center were used in this research.

APPENDIX

We define the following variables for the ensuring discussion.

(1) $P_c^{\parallel}$ is the momentum of the π^+ in the D^{*+} rest frame, for $D^{*+} \to D^0 \pi^+$, along the direction of motion of the D^{*+}.

(2) $P_c^{\perp}$ is the transverse momentum of the π^+, in the D^{*+} rest frame, for $D^{*+} \to D^0 \pi^+$, with respect to the direction of motion of the D^{*+}.

(3) $P_l^{\parallel}$ and $P_l^{\perp}$ are the corresponding momentum components in the laboratory frame. E_l is the energy of the π^+ in the laboratory frame.

(4) $\gamma = E_{D^{*+}}/M_{D^{*+}}$, where $E_{D^{*+}}$ and $M_{D^{*+}}$ refer to the energy and momentum of the D^{*+}. Also $\beta = P_{D^{*+}}/M_{D^{*+}}$, where $P_{D^{*+}}$ is the momentum. $\hat{\eta}$ refers to the unit vector along the thrust axis (which is taken to be the direction of $P_{D^{*+}}$).

With the definitions in (1) and (2), we can write the total center of mass (c.m.) and laboratory momentum of the π^+ as $\mathbf{P}_c = \mathbf{P}_c^{\parallel} + \mathbf{P}_c^{\perp}$, and $\mathbf{P}_l = \mathbf{P}_l^{\parallel} + \mathbf{P}_l^{\perp}$, respectively. The Lorentz transformations relating the c.m. and the laboratory frame can be written as

$$P_c^{\parallel} = \gamma(P_l^{\parallel} - (\beta \cdot \hat{\eta}) E_l) , \tag{A1}$$

$$P_c^{\perp} = P_l^{\perp} \equiv \sqrt{P_l^2 - P_l^{\parallel 2}} , \tag{A2}$$

where

$$P_l^{\parallel} = \mathbf{P}_l \cdot \hat{\eta} . \tag{A3}$$

Now,

$$P_c^{\parallel 2} + P_c^{\perp 2} = P_c^2 . \tag{A4}$$

Substituting Eqs. (A1), (A2), and (A3) into (A4), we get

$$\beta^2 (P_l^{\parallel})^2 + E_l^2 - P_l^2 + P_c^2) - 2E_l \beta P_l^{\parallel} + (P_l^2 - P_c^2) = 0 . \tag{A5}$$

Solving Eq. (A5) gives us two values for β. We then choose one value as explained in the text.

[1] For instance, see the following and the references contained within: N. Isgur, D. Scora, B. Grinstein, and M. B. Wise, Phys. Rev. D **39**, 799 (1989); N. Isgur and D. Scora, *ibid.* **40**, 1941 (1989); F. J. Gilman and R. L. Singleton, *ibid.* **41**, 142 (1990).

[2] J. G. Körner and G. A. Schuler, Z. Phys. C **38**, 511 (1988); **41**, 690(E) (1989).

[3] J. C. Anjos *et al.*, Phys. Rev. Lett. **62**, 722 (1989); **65**, 2630 (1990).

[4] Z. Bai *et al.*, Phys. Rev. Lett. **66**, 1011 (1991).

[5] D. Andrews *et al.*, Nucl. Instrum. Methods **211**, 47 (1983); D. G. Cassel *et al.*, *ibid.* **252A**, 325 (1986).

[6] R. Fulton *et al.*, Phys. Rev. D **43**, 651 (1991).

[7] G. C. Fox and S. Wolfram, Phys. Rev. Lett. **41**, 1581 (1978).

[8] For details, see S. Behrends *et al.*, Phys. Rev. Lett. **59**, 407 (1987); R. Kowaleski, Ph.D. thesis, Cornell University, 1987.

[9] We estimate that roughly 75% of the D^{*+}'s in the continuum are produced with momentum greater than 2 GeV/c; see D. Bortoletto *et al.*, Phys. Rev. D **37**, 1719 (1988).

[10] N. Isgur *et al.*, Phys Rev. D **39**, 799 (1989).

[11] We investigated the single-pole form-factor model of Körner and Schuler [2] and found the efficiencies to be consistent with the model of Isgur *et al.* [10].

[12] If we use the E691 result for the ratio of longitudinally polarized to transversely polarized K^{*-} of 1.8, we obtain an average efficiency of 0.92%.

[13] Note that real $D^{*+} \to \pi^+ D^0$, $D^0 \to K^{*-} e^+ \nu_e$ events from B decay are not considered background but part of the signal.

[14] We have also looked for decays with muons as well as electrons. Folding the shape of the lepton spectrum with the electron and muon efficiencies we expect to observe $\frac{1}{4}$ as many muons as electrons. We find 11 ± 7 muons. Since we have 54 ± 12 electrons we would have expected to see 13.5.

[15] This is consistent with the Mark III result where the search for unexpected semileptonic decay modes of the D^0 did not yield a positive result. See Ref. [4].

[16] As a check, we did the analysis requiring a much stricter tag on the kaon. In addition to requiring that the dE/dx loss for the kaon candidate be within 2σ of that expected for a kaon, we also require that the dE/dx loss for it be at least 2σ away from that expected for a pion. The results are consistent with ones quoted in the text.

[17] J. Adler *et al.*, Phys. Rev. Lett. **60**, 89 (1988).

[18] Particle Data Group, J. J. Hernández *et al.*, Phys. Lett. B **239**, 1 (1990).

[19] J. Adler *et al.*, Phys. Lett. B **196**, 107 (1987).

[20] J. C. Anjos *et al.*, Phys. Rev. Lett. **62**, 1587 (1989).

[21] The background shapes are determined using both Monte Carlo simulations and the data itself. The q^2 distribution for the lepton fakes is obtained from the data, whereas all other background shapes are obtained from Monte Carlo simulations.

[22] F. Bletzacker, H. T. Nieh, and A. Soni, Phys. Rev. **16**, 732 (1977); see also S. Stone, in *CP Violation,* edited by C. Jarlskog (World Scientific, Singapore, 1989).

[23] T. M. Aliev *et al.*, Yad. Fiz **40**, 823 (1984) [Sov. J. Nucl. Phys. **40**, 527 (1984)], predict 0.6 ± 0.1; Isgur *et al.* [1] predict 0.82; M. Bauer, B. Stech, and M. Wirbel, Z. Phys. C **29**, 637 (1985), predict 0.76, while C. A. Dominguez and N. Paver, Phys. Lett. B **207**, 199 (1988), predict 0.75.

[24] The model of Isgur *et al.* predicts the ratio of Cabibbo-suppressed to Cabibbo-favored modes to be 5%, whereas models which use a single-pole form factor predict this ratio to be roughly 10%. The second error in the estimate of Cabibbo-suppressed modes is due to this theoretical uncertainty.

[25] R. M. Baltrusaitis *et al.*, Phys. Rev. Lett. **54**, 1976 (1985).

[26] H. Albrecht *et al.*, Phys. Lett. B **255**, 634 (1991).

[27] K. Kodama *et al.*, Phys. Rev. Lett. **66**, 1819 (1991).